

Optimizing lens-coupled digital radiographic imaging systems based on model observers' performance

Liyang Chen^a, Harrison H. Barrett^{a,b,c}

^aOptical Sciences Center, ^bRadiology department, ^cApplied Mathematics Program,
University of Arizona, Tucson, AZ 85721

ABSTRACT

Recent advances in model observers that predict human perceptual performance now make it possible to optimize medical imaging systems for human task performance. We illustrate the procedure by considering the design of a lens for use in an optically coupled digital mammography system. The channelized Hotelling observer is used to model human performance, and the channels chosen are differences of Gaussians (DOGs). The task is detection of a lesion at a random but known location in a clustered lumpy background mimicking breast tissue. The entire system is simulated with a Monte Carlo application according to the physics principles, but the main system component under study is the lens that couples a fluorescent screen to a CCD detector. The bigger the aperture is, the larger the portion of light is coupled to the CDD, but the more severe the aberrations are, so the worse the image blur is. So when changing the stop size, the signal (lesion) detectability of human observers associated with this task also changes. The SNR of the channelized Hotelling observer is used to quantify this detectability. In this paper, plots of channelized Hotelling SNR vs. signal location for various lens apertures and working distances are presented. These plots thus illustrate the tradeoff between coupling efficiency and blur in a task-based manner. In this way, the channelized Hotelling SNR is used as a merit function for lens design.

Keywords: channelized Hotelling observer, lens design, digital mammography, clustered lumpy background

1. INTRODUCTION

Optical design today is an iterative optimization process, whose optimization criterion is usually to find a local minimum of a user-defined merit function. The typical merit function is the weighted sum of the squares of many image defects, such as various aberration terms. These terms are only loosely related to the quality of the image. When an image is produced for some specific purpose or task, such as a medical image, the only meaningful measure of the image quality is the appropriate observer's performance on that specific task. Recent advances in model observers that predict human perceptual performance now make it possible to optimize optical imaging systems, such as imaging lenses, for human task performance. The model observer's performance is considered as the objective measure of the image quality in the sense that there are no individual design choices involved, such as the weight coefficients in the merit function for lens design.

We illustrate the procedure by investigating the design of a lens for use in a digital mammographic imaging system. One type of these imaging systems uses an optical coupling approach between the fluorescent screen and the camera without image intensification. Both fiber-optic-coupled and lens-coupled CCD x-ray imaging systems have been developed for use in digital mammography and digital radiography¹⁻³. The cascaded imaging chain consists of a fluorescent screen, an optical coupling component, and an electronic imaging device, such as a CCD imager.

It is well known that severe limitations are associated with the optical coupling of an x-ray fluorescent screen to a digital image-capturing device. In this approach, a second quantum sink occurs at the optical coupling component because of the low optical coupling efficiency. In recent years, developments in high-sensitivity image sensors such as CCDs and lenses or reflective optics with high numerical aperture have prompted a re-examination of the optical coupling approach in digital mammographic imaging. The design criterion of the optical coupling components is mainly focused on overcoming the second quantum sink. Designers usually try to open up the aperture as large as possible while constraining aberrations under a certain amount. The purpose of this stringent design practice is to improve the image quality, but the definition of a good image is rather vague. Although every measure of final images indicates an aspect of

the image quality, such as the image blur and the image flux, each designer treats those measures in different ways based on their own understanding of the system and experience from previous designs. Even the balancing among different measures is not clear or uniform among different designs.

A clear and unified quantitative assessment of image quality is the solution to the above uncertainty. The measure of a specific observer's performance on a specific task can be this definition of image quality. There are generally two kinds of tasks: classification and estimation. In our mammographic systems case, images are first used to determine the presence of lesions, which belongs to classification category. There also exist several types of observers. Human observers like physicians are the most common observers to performance the lesion detection task. Because of the limitation of resources, it's difficult to estimate the human's performance at a reasonable accuracy. Due to recent advances in the studies of human vision systems and signal processing techniques, we can model human observers by a channelized Hotelling observer. With some knowledge of the statistics of objects being imaged and imaging systems under investigation, the signal-to-noise ratio (SNR) can be computed as the quantitative measure of the channelized Hotelling observer's performance. This figure of merit is thus used as a merit function in optimizing the optical coupling component design. All aspects of image qualities are unified in this single SNR. The individual feeling about balance between blur and flux can now be clearly quantified.

2. MODELING

2.1 Physical system description

The schematic system under investigation is a lens-coupled x-ray mammography imaging system (Fig. 1). The x-ray generator is in front of the fluorescent screen, and the objects being imaged are placed between the x-ray source and the screen. The imaging unit after the screen consists of a lens and a CCD camera. The lens images the exit surface of the screen onto the detector surface of the CCD camera.

The distance between the x-ray generator and the screen is assumed to be large compared to the size of the target so that the x-ray source can be safely treated as a point source. Also, the size of the screen is assumed to be small compared to this distance so that the x-ray beams from the target onto the screen are approximately parallel. Because the peak wavelength is extremely short compared with its broad wavelength range, the x-ray source is essentially completely incoherent. All of above approximations guarantee a satisfactory model of the x-ray beams from the source: a group of x-ray photons moving in the same direction during the exposure time interval.

X-ray fluorescent screens are usually made of rare-earth-doped polycrystalline materials, in plastic binders. These polycrystalline materials can emit visible light upon x-ray excitation. Terbium-doped crystals mainly emit green light when activated, which is the wavelength used in this work. The conversion number is random for every absorbed x-ray photon, while the ensemble average is around a thousand optical photons per x-ray photon. On the other hand, these tiny crystal grains serve as scattering centers for visible light propagating inside the screen, so from a single absorption position inside the screen, the outgoing photons have random displacement from the position projected on the exit surface of the screen. The outgoing directions of visible light photons are also randomly deviated from the unscattered direction defined by the absorption position and exit position on the screen surface. The imaging lens thus captures a small portion of the outgoing visible light inside its aperture and images it onto the CCD detector surface. The accepted portion is so small that the final x-ray to visible light conversion ratio can hardly reach 1! At the same time, the lens introduces aberrations that further blur final images on the CCD camera. The larger the aperture is, the more light hits the CCD camera, but the more severe the aberrations and thus the more blur in the image. The question is: where is the balancing point between these two factors?

The CCD camera can have very low noise and very sensitive response due to the current technology. For this paper, we assume an ideal noiseless CCD camera with an identical response function for every pixel. We can always take account of the electronic noise of the CCD camera later because this noise has a different physical mechanism and thus is independent of the photon noise.

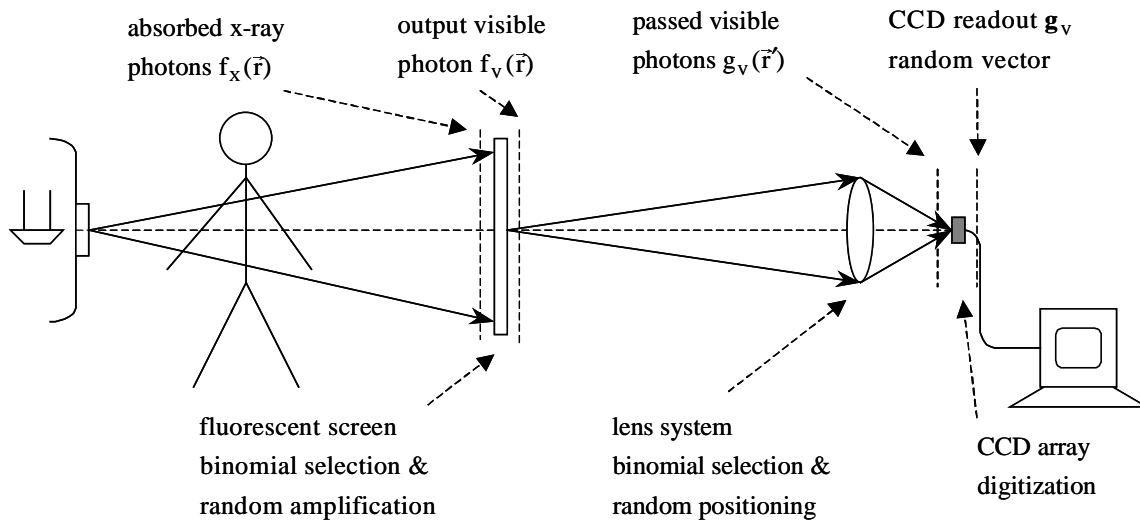


Fig 1. Layout of the simulated system

2.2 Mathematical system modeling

The physical descriptions and reasonable approximations form a very good starting point for mathematical modeling of the problem. From the start, the x-ray photons generated during the exposure time can be treated as a two-dimensional (2D) spatial stochastic point process. After passing through any given object being imaged, some of the x-ray photons are absorbed. This absorption mechanism acts as a binomial selection on the starting Poisson process, and the resulting process is still Poisson. After going through the fluorescent screen, a portion of x-ray photons are absorbed and converted into visible light photons. Only the visible light contributes to the final image on the CCD camera, because the unabsorbed x-ray photons also pass through the folding mirror that reflects visible light beams. So we merely need to consider the group of x-ray photons that are absorbed into the screen. This group is again a binomial selection of the original Poisson process, therefore also a Poisson point process. The mean of the process is a continuous 2D function acting as an object in front of the imaging system considered. Our mathematical model actually starts from this object with respect to our imaging system.

The first element encountered in the imaging chain is the fluorescent screen. This screen has two functions: amplification and scattering. All of the visible light photons produced by one x-ray photon can be approximately considered as first starting out from the same position as the x-ray absorption site, but going into isotropically random directions. Then, after being scattered by many tiny crystal grains, most of the visible light photons push their ways up to the exit surface of the screen. On this surface, those photons are all randomly displaced from the center position, which is the projection of the starting position on the exit surface along the incoming direction of the x-ray photon. The spatial part of these two steps can be precisely modeled as a type of random amplification mechanism acting on the starting Poisson point process⁴. This mechanism can be completely determined by a point spread function $p_d(\vec{r}, \vec{R}/z)$, where \vec{R} is the primary position, \vec{r} is the secondary position and z is the absorption depth, and $pr(k)$ is the probability density function (PDF) of the gain k . Because any well-manufactured screen should give the same response to an incoming x-ray photon anywhere not too close to the edges, the point-spread function p_d varies as the difference of its arguments, i.e. $p_d(\vec{r}, \vec{R}/z) = p_d(\vec{r} - \vec{R}/z)$. The propagation directions of the visible photons are also randomly deviated from the unscattered direction. The angular part of the two steps is described by a set of probability density functions on the propagation direction at every position on the exit surface of the screen $pr(\hat{s}/\vec{r}, \vec{R}, z)$, where \hat{s} is a unit vector within the forward hemisphere. The resultant 2D spatial point process right after the screen is no longer a Poisson one because the visible photons produced by the same x-ray photon are no longer independent of each other.

The angular randomness of the optical photons comes into play with the subsequent imaging lens. This lens also acts in two ways: letting a small portion of the visible photons pass through and deviating each passed photon from its ideal image point. If the emerging position and the outgoing direction of each photon are known on the exit surface of the screen, one will readily know whether this photon will pass the lens and where it hits on the CCD detector surface after going out of the lens. In fact, the lens performs deterministically instead of stochastically. Only when the propagation direction of a photon is random from a point on the exit surface of the screen can the lens be treated statistically. The imaging lens actually translates the angular randomness of incoming photons to the spatial randomness of outgoing photons. Therefore, the point-response function $p_g(\vec{r}', \vec{r} | z)$ of the same lens is different for the incoming light beams with different angular spread $pr(\hat{s} / \vec{r}, \vec{R}, z)$. Similarly, the portion of the incoming light that passes through the lens and hits the CCD detector varies according to $pr(\hat{s} / \vec{r}, \vec{R}, z)$. This portion equals the probability $pass(\vec{r}, \vec{R} / z)$ that a visible photon generated by an x-ray photon absorbed at position \vec{R} and depth z then emitting from the point \vec{r} on the exit surface of the screen can pass through the lens and hit the CCD detector. The first function of the lens is again a binomial selection mechanism. Then all the passed photons are displaced according to the point-response function $p_g(\vec{r}', \vec{r} / z)$, which is the result of the aberrations of the lens. The shift-invariance is broken because the aberrations with the large-aperture lens are highly field dependent. The second function of the lens is thus a special type of random amplification mechanism with the deterministic gain equaled one. After the lens, the 2D point process is on the detector surface of the CCD camera.

The last component in the imaging system is the CCD camera. With our ideal model, it simply bins the visible photons into each pixel without any additional noise. Thus the digital image is a random vector, with the noise determined by all of the random processes described above (but without electronic noise).

2.3 Model observer

Mathematical observers can be used to perform any specific task on this mathematically complete description of the imaging system. In particular, channelized Hotelling observers are able to predict the human perceptual performance in some specific tasks⁶, such as signal-known-exactly (SKE) classification tasks. When the signal position is variable but known to the observer, a plot of the figure of merit (FOM) versus the signal position can be used to describe the performance of the observer on this task.

Any mathematical model observer on the classification task is defined by a response function on the image vector $\lambda = w(\mathbf{g})$. For linear observers, $\lambda = \mathbf{w}^t \mathbf{g}$, where \mathbf{w} is a vector template applied on image vectors. In case of two-hypothesis classification tasks, or binary classification in other words, mathematical observers compare the response with a threshold λ_0 to make the decision. Our lesion-detection task is one example of binary classification tasks, with one hypothesis as lesion present and the other as lesion absent. We refer to lesions as signals in our study. The signal-present hypothesis is denoted as H_1 , while the signal-absent hypothesis is H_0 .

The signal-to-noise ratio (SNR) is one measure of observer's performance, given in terms of the mean and the variance of λ under both hypotheses. It is defined as

$$SNR^2 = \frac{[\langle \lambda | H_1 \rangle - \langle \lambda | H_0 \rangle]^2}{\frac{1}{2}(\sigma_1^2 + \sigma_0^2)},$$

where σ_1 and σ_0 are the variances of λ under the signal-present and signal-absent hypotheses respectively. For linear observers, the SNR is

$$SNR^2 = \frac{\left[\mathbf{w}^t (\langle \mathbf{g} | H_1 \rangle - \langle \mathbf{g} | H_0 \rangle) \right]^2}{\mathbf{w}^t \left(\frac{1}{2} \mathbf{K}_{g,1} + \frac{1}{2} \mathbf{K}_{g,0} \right) \mathbf{w}},$$

where $\mathbf{K}_{g,1}$ and $\mathbf{K}_{g,0}$ are the covariance matrices of the image vector under both hypotheses respectively.

The Hotelling observer is the ideal linear observer in the sense of maximum signal-to-noise ratio (SNR) among all linear observers. Its template is $\mathbf{w}_{Hotelling} = \mathbf{K}_g^{-1} \Delta \bar{\mathbf{g}}$, where $\Delta \bar{\mathbf{g}} = \langle \mathbf{g} | H_1 \rangle - \langle \mathbf{g} | H_0 \rangle$. Therefore the Hotelling observer's signal-to-noise ratio is as follows

$$SNR^2 = \Delta \bar{\mathbf{g}}^t \bar{\mathbf{K}}^{-1} \Delta \bar{\mathbf{g}},$$

where $\bar{\mathbf{K}} = \frac{1}{2} \mathbf{K}_{g,1} + \frac{1}{2} \mathbf{K}_{g,0}$.

The notion of channels in the human visual system has been studied intensively in vision science for many years⁶⁻⁸. The application of the channelized observers to medical image-quality assessment began not as long ago⁹. A channelized Hotelling observer performs a classification task after first reducing the image to a smaller set of channel response variables, defined by the transformation $\mathbf{u} = \mathbf{T}^t \mathbf{g}$, where the column vectors of the matrix \mathbf{T} each represent the spatial profile of a channel. If we postulate that the channel responses are transformed into a scalar observer response variable via Hotelling strategy, then the formula for observer SNR is given as

$$SNR_{ch}^2 = \Delta \bar{\mathbf{g}}^t \mathbf{T} (\mathbf{T}^t \bar{\mathbf{K}} \mathbf{T})^{-1} \mathbf{T}^t \Delta \bar{\mathbf{g}}.$$

The whole image is composed of both the signal and background in the signal-present case and only background in the signal-absent case, together with the fore-mentioned complicated noises. We consider a SKE situation where the signal profile is a deterministic 2D function. The background in mammography is usually a complex texture that can be satisfactorily modeled by a mathematical 2D function called a clustered lumpy background¹⁰. Because the objects being imaged will be from more than one patient, the background is random. When considering the random background, the group of x-ray interactions in our system model is not a Poisson random process but a doubly stochastic Poisson random process with random mean. The ensemble average taken in the SNR_{ch} formula should be done over both the Poisson process conditioned on a given background and the random backgrounds themselves. With all the knowledge on the object, the imaging system and the model of the observer, the measure of the image quality is written as

$$SNR^2 = \bar{\mathbf{g}}_s^t \mathbf{T} (\mathbf{T}^t \bar{\mathbf{K}} \mathbf{T})^{-1} \mathbf{T}^t \bar{\mathbf{g}}_s,$$

where $\bar{\mathbf{g}}_s$ is the mean image vector of the signal and $\bar{\mathbf{K}}$ is the overall covariance matrix of the image ensemble. The mean image vector is as follows

$$\bar{g}_s^i = \iint d^2 r' h_i(\vec{r}') \iint d^2 R s(\vec{R}) p_i(\vec{r}', \vec{R}) \quad i = 1, \dots, N$$

where \bar{g}_s^i is the i^{th} element of $\bar{\mathbf{g}}_s$. The signal profile is $s(\vec{R})$ on the exit surface of the screen. The response function of the i^{th} pixel $h_i(\vec{r}')$ is a small rectangular function centered at the pixel on the CCD detector plane. We will explain the total point-response function $p_i(\vec{r}', \vec{R})$ later in this section. The overall covariance matrix $\bar{\mathbf{K}}$ is the sum of three separate terms, including the contributions from Poisson statistics of the x-ray photons, the random acceptance of the optical photons into the image and the object randomness.

$$\bar{\mathbf{K}}_{ij} = \bar{\mathbf{K}}_{ij}^{(1)} + \bar{\mathbf{K}}_{ij}^{(2)} + \bar{\mathbf{K}}_{ij}^{(3)} \quad i = 1, \dots, N \ \& \ j = 1, \dots, N$$

$$\bar{\mathbf{K}}_{ij}^{(1)} = \delta_{ij} \iint d^2 r' h_i(\vec{r}') \iint d^2 R \left(\bar{b}(\vec{R}) + \frac{1}{2} s(\vec{R}) \right) p_t(\vec{r}', \vec{R})$$

$$\bar{\mathbf{K}}_{ij}^{(2)} = \iiint d^2 r'_1 d^2 r'_2 h_i(\vec{r}'_1) h_j(\vec{r}'_2) \int_0^d dz \alpha_x e^{-\alpha_x z} Q(\vec{R}, z) \iint d^2 R \left(\bar{b}(\vec{R}) + \frac{1}{2} s(\vec{R}) \right) p_t(\vec{r}'_1, \vec{R} | z) p_t(\vec{r}'_2, \vec{R} | z)$$

$$\bar{\mathbf{K}}_{ij}^{(3)} = \iiint d^2 r'_1 d^2 r'_2 h_i(\vec{r}'_1) h_j(\vec{r}'_2) \iint \iint d^2 R_1 d^2 R_2 K_b(\vec{R}_1, \vec{R}_2) p_t(\vec{r}'_1, \vec{R}_1) p_t(\vec{r}'_2, \vec{R}_2)$$

where α_x is the x-ray absorption of the fluorescent screen and d is the screen thickness. The ensemble mean background is $\bar{b}(\vec{R})$, and the covariance function of the background is $K_b(\vec{R}_1, \vec{R}_2)$. From the expression of the clustered lumpy background, we have the analytical form of the two moments of the background used in the SNR calculation. The function $Q(\vec{R}, z)$ involves the first and the second moments of the random gain k of the screen. The function is defined as $Q(\vec{R}, z) = \frac{\overline{k^2} - \bar{k}}{\bar{k}^2}$. Though we don't know the probability density function of k , we do have the knowledge of the average gain and the variance of gain if we know the Swank factor. Both the total point spread function $p_t(\vec{r}', \vec{R})$ and the point spread function $p_t(\vec{r}', \vec{R} | z)$ conditioned on the absorption depth are derived from the mathematical description of the system:

$$p_t(\vec{r}', \vec{R}) = \int_0^d dz \alpha_x e^{-\alpha_x z} p_t(\vec{r}', \vec{R} | z)$$

$$p_t(\vec{r}', \vec{R} | z) = \iint d^2 r p_d(\vec{r}, \vec{R} | z) p_{ass}(\vec{r}, \vec{R} | z) p_g(\vec{r}', \vec{r} | \vec{R}, z)$$

With all the necessary expressions and parameters at hand, the simulation can be done to evaluate the SNR of the system.

2.4 Numerical calculation

We should not get lost in the messy expression above. Instead, the formula shows a separation in the system information and the object variation. The system is all encapsulated into the total point spread function and the Q function, while objects express themselves in the ensemble mean and the covariance functions of backgrounds and deterministic signals.

A Monte Carlo application is used to compute the SNR numerically. Because of the shift-variant property of the lens imaging process, we don't use an approximate point response function to model the lens. Instead, a numerical ray-tracing code is exploited in the Monte Carlo simulation to actually trace rays through the lens. Both the passing probability of a visible light photon and the aberration on the image plane are precisely taken into account by the ray-tracing code.

3. RESULTS

The system being investigated is a small-view mammography imaging system. The signal is chosen as a small Gaussian blob with the peak value at 10% of the mean background. The standard deviation of the Gaussian signal profile is 0.5 millimeter. The x-ray absorption coefficient of the screen is 0.13 mm^{-1} , and the screen is 84 microns thick. The CCD pixel is square and 50 microns on a side. The detector array of the CCD camera is 128 by 128 without gaps between adjacent pixels. The screen being imaged is larger than the camera's field of view so that the edge effects from the screen can be neglected. The lens being modeled is deliberately a poor design so that we can compare the effect of aberrations with the effect of the aperture.

A plot of SNR vs. signal position at different aperture sizes is presented in Fig. 2. The bigger the aperture, the larger portion of light is coupled onto the CCD, but the more severe the aberrations are, so the worse the image blur. When the aperture is opened up, the SNR first increases because of the increased portion of light that gets through the lenses. When the aperture is opened further, more aberrations are added to the images and the images are blurred by a wider point response function. The effect of the aberrations manifests itself by slowing down the increment of SNR until it reaches a maximum. Then with even larger aperture, the SNR begins to decrease. Although we cannot open the aperture further in this design, the plot illustrates the existence of the maximum SNR. It shows the tradeoff between coupling efficiency and blur in an objective, task-based manner.

A plot of SNR vs. signal position at different working distances is presented in Fig.3. Sometimes lenses may be used in the conjugate position other than its designed one. We investigate the working distance effect in task-based manner as well. The lens aperture is at an object-space numerical aperture of 0.055, when the magnification is -0.10 . Then the screen is imaged at different magnifications but fixed aperture size. The shorter the working distance become, the larger is the magnification. However, the aberration is worsened because the lens is used away from its designed position. We find in the Fig. 3 below that the observer's performance decreases significantly with the increased deviation from the designed conjugate position of the lenses.

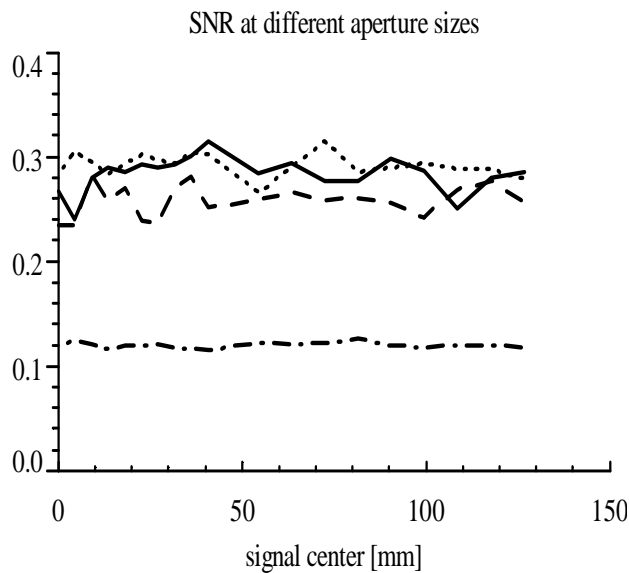


Fig 2. SNR vs. signal positions at different aperture sizes. The signal positions are measured on the exit surface of the screen. The aperture sizes are measured in terms of numerical apertures in object space: $NA = 0.055$ is plotted in solid line, 0.45 in dotted line, 0.35 in dashed line and 0.010 in dash-dotted line.

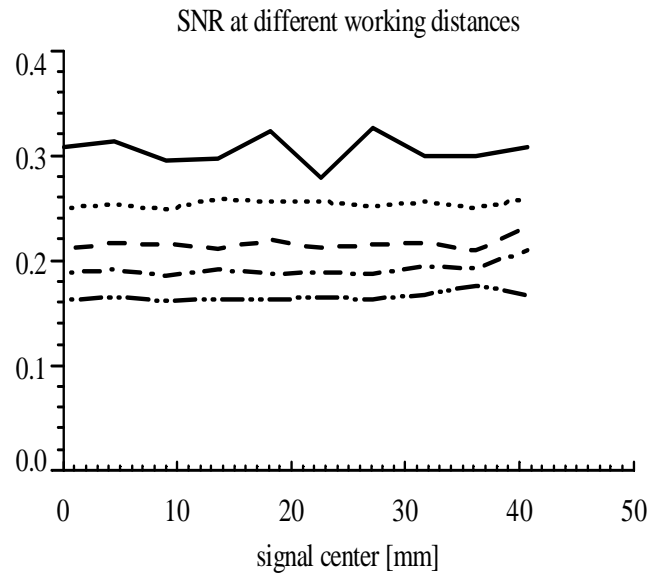


Fig 3. SNR vs. signal positions at different working distances. The signal positions are measured on the exit surface of the screen. The working distances are measured in terms of the magnifications: $M = -0.1$ is plotted in solid line, -0.11 in dotted line, -0.12 in dashed line, -0.13 in dash-dotted line and -0.14 in dash-dot-dotted line.

4. DISCUSSION AND CONCLUSIONS

To the authors' knowledge, this paper is the first to use a perception-based detectability measure as a figure of merit for lens design. This system-evaluation technique explicitly connects the optical coupling efficiency with the aberration-based blur in an objective, task-based manner, independent of the designer's experiences. Based on this criterion, we can investigate the tradeoff between the aberrations and the light loss in optically coupled mammographic imaging systems.

Design of optical imaging systems can be done based on objectively defined signal-to-noise ratio of the model observers instead of the subjectively built merit functions. In stringent design requirements like medical imaging, the

observers' performance is a good tool for evaluating the system quality for some task. There are several object models and observer models suitable for mammographic imaging systems in tumor detection tasks, and they can serve as a good starting place to apply task-based design techniques.

5. ACKNOWLEDGEMENTS

The authors would like to thank E. Clarkson for useful discussions. This work was made possible by funding from the National Institute of Health grants RO1 CA52643 and R37 EB 000803.

REFERENCES

1. Andrew Karellas and Lisa J. Harris, Hong Liu, Michael A. Davis and Carl J. D'Orsi, "Charge-coupled device detector: performance considerations and potential for small-field mammographic imaging applications", *medical physics*, **19**(4), pp 1015-23, 1992
2. Aparna Visweswaran, Hong Liu, Laurie L. Fajardo and Gia A. DeAngelis, "Comparison of contrast detail curves of full field digital with screen film breast phantom images", *Frontiers in Bioscience*, **1**, pp 5-7, 1996
3. Andrew D. A. Maidment, Martin J. Yaffe, Donald B. Plewes, Grodon E. Mawdsley, Ian C. Soutar and Brian G. Starkoski, "Imaging performance of a prototype scanned-slot digital mammography system", *Proc. SPIE*, **1896**, pp 93-103, 1993
4. Harrison H. Barrett and Kyle J. Myers, *Foundations of Image Science*, John Wiley & Sons, 2003
5. Craig K. Abbey and Harrison H. Barrett, "Human- and model-observer performance in ramp-spectrum noise: effects of regularization and object variability", *Journal of Optical Society of America A*, **18**(3), pp 473-88, 2001
6. F. W. Campbell and J. G. Robson, "Application of Fourier analysis to the visibility of gratings", *Journal of Physiology*, **197**, pp 551-66, 1968
7. M. B. Sachs, J. Nachmias and J. G. Robson, "spatial frequency channels in human vision", *Journal of the Optical Society of America*, **61**, pp 1176-86, 1971
8. Norma Graham, "complex channels, early nonlinearities, and normalization in texture segregation", *Computational Models of Visual Processing*, M. S. Landy and J. V. Movshon, MIT press, Cambridge, MA, pp 273-90, 1990
9. Kyle J. Myers and Harrison H. Barrett, "The addition of a channel mechanism to the ideal-observer model", *Journal of the Optical Society of America*, **4**, pp 2447-57, 1987
10. Francois O. Bochud, Craig K. Abbey and Miguel P. Eckstein, "Statistical texture synthesis of mammographic images with clustered lumpy backgrounds", *Optical express*, **4** (1), pp 33-43, 1999